Polymorphism and Related Magnetic Behavior in Decamethylferrocenium Salts of Transition-Metal Maleonitriledithiolates

Mohammed Fettouhi,[1a] Lahcène Ouahab,*[1a] Massa Hagiwara,[1b] Epiphane Codjovi,[1b] Olivier Kahn,*[1b] H. Constant-Machado,[1c] and François Varret[1c]

Laboratoire de Chimie du Solide et Inorganique Moléculaire, URA/CNRS 1495, Université de Rennes I, 35042 Rennes cédex, France, Laboratoire de Chimie Inorganique, URA/CNRS 420, Université de Paris Sud, 91405 Orsay, France, and Laboratoire d'Optique et Magnétisme, EP CNRS 0035, Université de Versailles, 78035 Versailles Cédex, France

Received December 22, 1994[⊗]

Several decamethylferrocenium/transition-metal maleonitriledithiolate compounds have been synthesized and structurally characterized. The compounds $[Fe(cp^*)_2]_x[M(mnt)_2]_y(CH_3CN)_z$ (M = Cu(II), Co(III), Fe(III)) crystallize in the triclinic space group $P\bar{1}$ (No. 2). For M = Co(III) two solid-state phases have been isolated. α-$[Fe(cp^*)_2]_2[Co(mnt)_2]_2(CH_3CN)_2$ (Fe_2Co_2A): $a = 9.894(4)$ Å, $b = 12.942(6)$ Å, $c = 15.056(6)$ Å, $\alpha = 110.13(3)°$, $\beta = 98.41(4)°$, $\gamma = 107.78(3)°$, $V = 1657$ Å^3, $M_r = 1413.3$, $d_c = 1.419$ g/cm^3, $Z = 1$, and $R = 0.061$ for 2351 reflections with $I \geq 3\sigma(I)$. β-$[Fe(cp^*)_2]_2[Co(mnt)_2]_2$ (Fe_2Co_2B): $a = 9.576(8)$ Å, $b = 12.849(4)$ Å, $c = 13.641(7)$ Å, $\alpha = 108.13(4)°$, $\beta = 90.91(6)°$, $\gamma = 103.54(4)°$, $V = 1544$ Å^3, $M_r = 1331.2$, $d_c = 1.431$ g/cm^3, $Z = 1$, and $R = 0.043$ for 2407 reflections with $I \geq 3\sigma(I)$. The isostructural α modification is observed for M = Fe(III). α-$[Fe(cp^*)_2]_2[Fe(mnt)_2]_2(CH_3CN)_2$ (Fe_2Fe_2A): $a = 9.905(7)$ Å, $b = 12.966(5)$ Å, $c = 15.142(3)$ Å, $\alpha = 109.77(2)°$, $\beta = 98.64(4)°$, $\gamma = 108.06(6)°$, $V = 1668$ Å^3, $M_r = 1407.2$, $d_c = 1.401$ g/cm^3, $Z = 1$, and $R = 0.063$ for 3125 reflections with $I \geq 3\sigma(I)$. The dimeric anionic species show a square pyramidal coordination for the metal (the apical M−S bonds are Co−S = 2.39, 2.35 Å and Fe−S = 2.49 Å). Orthogonal arrangement of adjacent cations is observed in the decamethylferrocenium chains of the two α compounds, while a parallel packing exists in the β modification. $[Fe(cp^*)_2]_2Cu(mnt)_2$ (Fe_2Cu): $a = 9.713(5)$ Å, $b = 11.407(4)$ Å, $c = 11.958(5)$ Å, $\alpha = 100.90(2)°$, $\beta = 113.20(5)°$, $\gamma = 92.66(3)°$, $V = 1185$ Å^3, $M_r = 996.5$, $d_c = 1.396$ g/cm^3, $Z = 1$, and $R = 0.041$ for 2724 reflections with $I \geq 3\sigma(I)$. The dianion $[Cu(mnt)_2]^{2-}$ exhibits a planar monomeric structure and the mixed anion−cation stacks adopt a $\cdots A^{2-}D^+D^+A^{2-}D^+D^+A^{2-}\cdots$ arrangement with short anion−cation distances: d(Fe−S) = 5.54 Å and d(Fe−Cu) = 6.37 Å. The magnetic properties of all the compounds have been investigated. In both Fe_2Co_2A and Fe_2Co_2B the decamethylferrocenium cations have been found to be magnetically isolated. In Fe_2Fe_2A, a strong antiferromagnetic interaction within the $\{[Fe(mnt)]_2\}^{2-}$ dimeric unit has been characterized. In Fe_2Cu, finally, each $[Cu(mnt)_2]^{2-}$ is found to interact antiferromagnetically with two adjacent $[Fe(C_p^*)_2]^+$ cations.

Introduction

Since the description in 1986 of bulk molecular magnets,[2,3] great efforts have been devoted to these kind of materials.[4,5] Among the strategies developed,[6] special attention has been given to the one based on charge transfer complexes. In fact, planar electronic acceptors (A) have been described to enable formation of such complexes with the $\cdots A^-D^+A^-D^+A^-\cdots$ structural sequence and support ferromagnetic behavior in the decamethylferrocenium-based salts.[7−11] In order to explore all prospects for such anions, monomeric and monoanionic planar metal−bis(dithiolene) complexes (M = Ni(III) and Pt(III)) have already been investigated and yield in most cases the $\cdots D^+A^-A^-D^+D^+A^-A^-D^+\cdots$ arrangement with an essentially eclipsed $S = 0$ [A^{2-}] ion and a thermally inaccessible triplet state.[8] Since the structural factor appears to be crucial for such systems, it was then convenient to investigate the structural richness and related magnetic behavior which could be afforded by special dianionic counterparts. Hence some decamethylferrocenium compounds based on planar bis(dithiolate) dianions have been obtained and the preparation, structure, and magnetic properties of the compounds $[Fe(cp^*)_2]_2Cu(mnt)_2$, α-$[Fe(cp^*)_2]_2[M(mnt)_2]_2(CH_3CN)_2$ [M = Co(III), Fe(III)], and β-$[Fe(cp^*)_2]_2[Co(mnt)_2]_2$ (mnt = $[S_2C_2(CN)_2]^{2-}$ (maleonitriledithiolate); cp* = pentamethylcyclopentadienyl) are reported.

Experimental Section

Preparation of Compounds. $NaFe(mnt)_2$,[12] $[(C_4H_9)_4N]Fe(mnt)_2$,[12] $[(C_4H_9)_4N]Co(mnt)_2$,[12] $[(C_4H_9)_4N]_2Cu(mnt)_2$,[12] $[Fe(Cp^*)_2]$,[13] and $[Fe(Cp^*)_2]BF_4$[13] were prepared and recrystallized by following the literature procedures. For all complexes the stoichiometries were determined by chemical analysis and X-ray crystal structure analysis.

α-$[Fe(cp^*)_2]_2[Co(mnt)_2]_2(CH_3CN)_2$ and $[Fe(cp^*)_2]_2Cu(mnt)_2$ were prepared by the same procedure: The reaction of stoichiometric

⊗ Abstract published in *Advance ACS Abstracts,* July 1, 1995.

(1) (a) Université de Rennes I. (b) Université de Paris Sud. (c) Université de Versailles.
(2) Miller, J. S.; Calabresse, J. C.; Epstein, A. J.; Bigelow, W.; Zhang, J. H.; Reiff, W. M. *J. Chem. Soc., Chem. Commun.* **1986**, 1026.
(3) Pei, Y.; Verdaguer, M.; Kahn, O.; Sletten, J.; Renard, J. P. *J. Am. Chem. Soc.* **1986**, *108*, 7428.
(4) Kahn, O. *Molecular Magnetism*; VCH: New York, 1993.
(5) *Research Frontiers in Magnetochemistry*; O'Connor, C. J., Ed.; 1994.
(6) Stumpf, H. O.; Ouahab, L.; Pei, Y.; Bergerat, P.; Kahn, O. *J. Am. Chem. Soc.* **1994**, *116*, 3866 and references therein.
(7) Miller, J. S.; Epstein, A. J.; Reiff, W. M. *Science* **1988**, *240*, 40.
(8) Miller, J. S.; Calabrese, J. C.; Epstein, A. J. *Inorg. Chem.* **1989**, *28*, 4230.
(9) Broderick, W. E.; Thomson, J. A.; Day, E. P.; Hoffman, B. M. *Science* **1990**, *249*, 401.
(10) Broderick, W. E.; Hoffman, B. M. *J. Am. Chem. Soc.* **1991**, *113*, 6334.
(11) Eichhorn, D. M.; Skee, D. C.; Broderick, W. E.; Hoffman, B. M. *Inorg. Chem.* **1993**, *32*, 491.
(12) Davison, A.; Holm, H. R. *Inorg. Synth.* **1967**, *10*, 8.
(13) Hendrickson, D. N.; Sohn, Y. S.; Gray, H. B. *Inorg Chem.* **1971**, *10*, 1559.

0020-1669/95/1334-4152$09.00/0

Table 1. Crystal Data for $[Fe(cp^*)_2]_x[M(mnt)_2]_y(CH_3CN)_z$

	$[Fe(cp^*)_2]_2[Co(mnt)_2]_2(CH_3CN)_2$	$[Fe(cp^*)_2]_2[Co(mnt)_2]_2$	$[Fe(cp^*)_2]_2[Fe(mnt)_2]_2(CH_3CN)_2$	$[Fe(cp^*)_2]_2[Cu(mnt)_2]$
formula	$Co_2Fe_2C_{60}H_{66}N_{10}S_8$	$Co_2Fe_2C_{56}H_{60}N_8S_8$	$Fe_4C_{60}H_{66}N_{10}S_8$	$CuFe_2C_{48}H_{60}N_4S_4$
fw	1413.3	1331.2	1407.2	996.53
space group	$P\bar{1}$ (No. 2)	$P\bar{1}$ (No. 2)	$P\bar{1}$ (No. 2)	$P\bar{1}$ (No. 2)
a, Å	9.894(4)	9.576(8)	9.905(7)	9.713(5)
b, Å	12.942(6)	12.849(4)	12.966(5)	11.407(4)
c, Å	15.056(6)	13.641(7)	15.142(3)	11.958(5)
α, deg	110.13(3)	108.13(4)	109.77(2)	100.90(2)
β, deg	98.41(4)	90.91(6)	98.64(4)	113.20(5)
γ, deg	107.78(3)	103.54(4)	108.06(6)	92.66(3)
V, Å^3	1654	1544	1668	1185
Z	1	1	1	1
T, K	298	298	298	298
λ(Mo Kα), Å	0.710 73	0.710 73	0.710 73	0.710 73
ϱ_c, g/cm^3	1.419	1.431	1.401	1.396
μ, cm^{-1}	12.09	12.89	11.37	12.56
R^a	0.061	0.043	0.063	0.041
$R_w{}^a$	0.082	0.054	0.088	0.060

^{a} $R = \Sigma(|F_o| - |F_c|)/\Sigma|F_o|$; $R_w = [\Sigma w(|F_o| - |F_c|)^2/\Sigma w|F_o|^2]^{1/2}$.

amounts of $[(C_4H_9)_4N]_nM(mnt)_2$ [M = Cu (n= 2), Co (n = 1)] and $[Fe(Cp^*)_2]BF_4$ in hot acetonitrile gave shiny black crystals which grew from the filtrate. The product was filtered out and washed with dichloromethane to remove the remaining starting compounds. Recrystallization from acetonitrile afforded nicely formed crystals. Anal. Obs (calc) for $Co_2Fe_2C_{60}H_{66}N_{10}S_8$: C, 50.78 (50.99); H, 4.71 (4.71); N, 9.37 (9.91); S, 18.01 (18.15); Co, 8.81 (8.34); Fe, 7.18 (7.90). Anal. Obs (calc) for $CuFe_2C_{48}H_{60}N_4S_4$: C, 57.99 (57.85); H, 6.05 (6.068); N, 5.80 (5.62); S, 12.73 (12.87); Cu, 6.35 (6.38); Fe, 10.50 (11.21).

β-$[Fe(cp^*)_2]_2[Co(mnt)_2]_2$. This compound was obtained by following the procedure described above using amounts of $[(C_4H_9)_4N]$-$Co(mnt)_2$ first treated by iodine to have complete metal oxidation in the starting salt.[12] Anal. Obs (calc) for $Co_2Fe_2C_{56}H_{60}N_8S_8$: C, 50.80 (50.53); H, 4.66 (4.54); N, 8.53 (8.42); S, 18.96 (19.27); Co, 8.73 (8.85); Fe, 8.17 (8.39).

α-$[Fe(cp^*)_2]_2[Fe(mnt)_2]_2(CH_3CN)_2$. To a boiling ethanol solution of $NaFe(mnt)_2$ was added a stoichiometric amount of $[Fe(Cp^*)_2]BF_4$ in hot ethanol. The dark precipitate was filtered out, washed with absolute ethanol and dichloromethane, and recrystallized from acetonitrile at low temperature (−18 °C) to give shiny black crystals. Anal. Obs (calc) for $Fe_4C_{60}H_{66}N_{10}S_8$: C, 51.16 (51.21); H, 4.59 (4.73); N, 9.54 (9.95); S, 18.30 (18.23); Fe, 15.19 (15.87).

Crystallographic Data Collection and Structure Determination. The X-ray data collections were performed on an Enraf-Nonius CAD4 diffractometer equipped with a graphite-monochromated Mo Kα (λ = 0.710 73 Å) radiation. The unit cell parameters were determined and refined from setting angles of 25 accurately centered reflections. Data were collected with the $\theta-2\theta$ scan method. Three standard reflections were measured every 1 h and revealed no fluctuations in intensities. Intensities were corrected for Lorentz and polarization effects. The structures were solved by direct methods and successive Fourier difference synthesis. An empirical absorption correction was applied using the DIFABS procedure.[14] The refinements (on F) were performed by the full-matrix least squares method [H atoms, both found by Fourier synthesis and placed at computed positions, were not refined]. The scattering factors were taken from *International Tables for X-ray Crystallography* (1974). All the calculations were performed on a MicroVAX 3100 using the Molen programs.[15]

The crystal data of all compounds are presented in Table 1. Selected bond lengths and bond angles are given in Table 2. Atom-labeling diagrams and thermal vibration ellipsoids and tables of atomic coordinates, bond lengths, bond angles, and anisotropic thermal parameters and are given as supporting information.

Mössbauer Spectroscopy. Transmission spectra have been recorded on a constant-acceleration spectrometer, using a 25 mCi ^{57}Co:Rh source. Typical instrumental line width is 0.22 mm s^{-1}. The sample contained ~70 mg of α-$[Fe(cp^*)_2]_2[Fe(mnt)_2]_2(CH_3CN)_2$, in the polycrystalline state, spread over a 2.5 cm^2 disk. The spectra were least squares fitted using the homemade MOSFIT program.[16]

Table 2. Selected Bond Distances and Bond Angles for the Compounds $[Fe(cp^*)_2]_x[M(mnt)]_y(CH_3CN)_z$

compd	bond distance (Å)		bond angle (deg)	
Fe_2Co_2A	Co−S1	2.181(4)	S1−Co−S2	91.2(1)
	Co−S2	2.173(4)	S1−Co−S3	90.1(1)
	Co−S3	2.187(4)	S1−Co−S4	176.3(1)
	Co−S4	2.188(3)	S2−Co−S3	157.6(1)
	Co−$S4_{ap}$	2.392(4)	S2−Co−S4	86.6(1)
			S3−Co−S4	90.7(1)
Fe_2Co_2B	Co−S1	2.191(2)	S1−Co−S2	87.22(7)
	Co−S2	2.174(2)	S1−Co−S3	175.19(9)
	Co−S3	2.180(2)	S1−Co−S4	90.66(8)
	Co−S4	2.193(2)	S2−Co−S3	91.30(8)
	Co−$S1_{ap}$	2.352(2)	S2−Co−S4	155.61(9)
			S3−Co−S4	88.80(8)
Fe_2Fe_2A	Fe−S1	2.223(1)	S1−Fe−S2	89.1(5)
	Fe−S2	2.216(1)	S1−Fe−S3	89.1(5)
	Fe−S3	2.222(1)	S1−Fe−S4	168.1(5)
	Fe−S4	2.219(1)	S2−Fe−S3	154.1(5)
	Fe−$S4_{ap}$	2.487(1)	S2−Fe−S4	86.1(5)
			S3−Fe−S4	89.1(5)
Fe_2Cu	Cu−S1	2.279(1)	S1−Cu−S2	90.67(5)
	Cu−S2	2.262(2)		

Magnetic Measurements. These were carried out with two instruments, namely a Faraday-type magnetometer working in the 4−300 K temperature range and a SQUID magnetometer working down to 1.7 K with magnetic fields up to 80 kOe.

Discussion

X-ray Crystal Structures. Structure of α-$[Fe(cp^*)_2]_2$-$[M(mnt)_2]_2(CH_3CN)_2$ [M = Co(III) (Fe_2Co_2A), Fe(III) (Fe_2Fe_2A)]. These two compounds are isostructural. Their crystal structures are represented in Figure 1. The $M(mnt)_2$ units form discrete dimers in which the metal assumes a quasi-square-pyramidal coordination as found in other binuclear metal−bis-(dithiolene) complexes.[17] In these molecules the displacement of the metal atom from the ligand plan to form M−S or M−M dimers depends on three main factors, namely the formation of new bonds between monomers, the pyramidalization of the metal atom, and finally the repulsion between the π electrons of both

(14) Walker, N.; Stuart, D. *Acta Crystallogr.* **1983**, *A39*, 158.
(15) Crystal Structure Analysis, Molecular Enraf-Nonius (MolEN), Delft Instruments X-ray Diffraction, B.V. Rontgenweg 1 2624 BD, Delft, The Netherlands, 1990.
(16) (a) Teillet, J.; Varret, F. Unpublished results. (b) Varret, F. Presented at the Intern. Conf. Applic. Mössbauer Effect (Jaïpur, India, 1981); proceedings pp 129−140.
(17) Alvarez, S.; Vicente, R.; Hoffman, R. *J. Am. Chem. Soc.* **1985**, *107*, 6253.

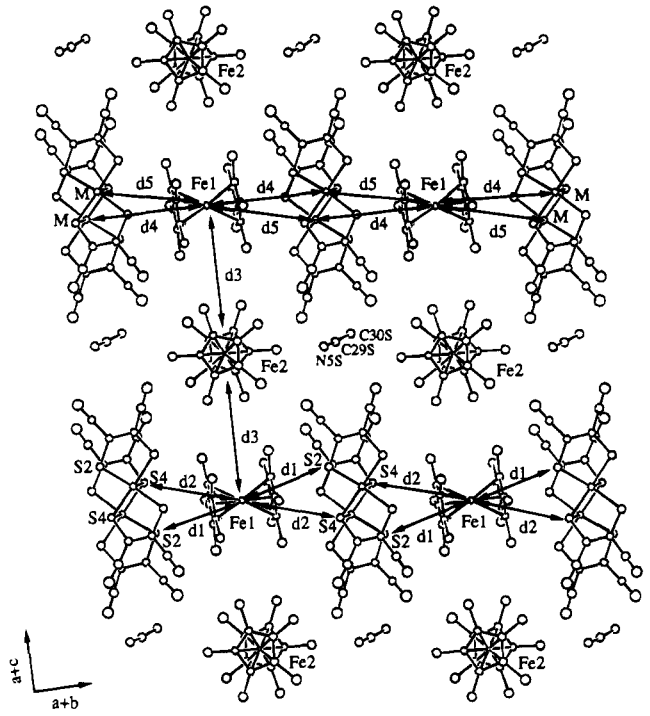

Figure 1. Structure of the Compounds α-$[Fe(cp^*)_2]_2[M(mnt)_2]_2(CH_3CN)_2$ [M = Co(III) and Fe(III)] with the shortest Fe−Fe, Co−Fe and Fe−S distances. M = Co: *d*1 = 5.297(3), *d*2 = 5.759(3), *d*3 = 8.382(1), *d*4 = 6.867(2), *d*5 = 7.169(2) Å. M = Fe: *d*1 = 5.317(2), *d*2 = 5.690(2), *d*3 = 8.402(1), *d*4 = 6.887(1), *d*5 = 7.118(1) Å.

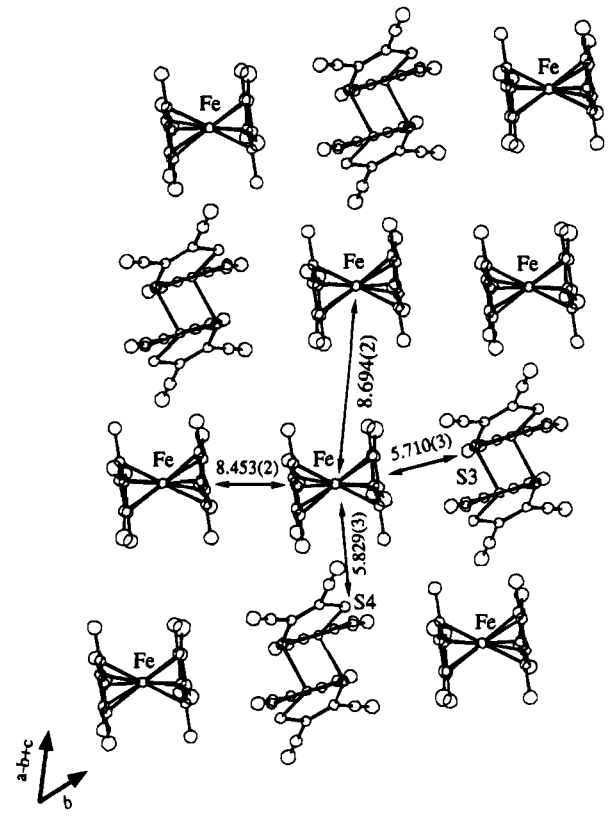

Figure 2. : Structure of the mixed one-dimensional stacks for β-$[Fe(cp^*)_2]_2[Co(mnt)_2]_2$ with the shortest Fe−Fe and Fe−S distances.

monomers.[17] The apical M−S bond length [M = Fe, 2.487(5) Å; M = Co, 2.392(5) Å] is somewhat longer than the four basal ones mean value [M = Fe, 2.221(5) Å; M = Co, 2.181(5) Å] as observed in $(Hpy)_2[M(mnt)_2]_2$,[18] $Co_2[S_4C_4(CF)_3]_2$,[19] and $(n\text{-}Bu_4N)_2[Co(S_2C_6Cl_4)_2]_2$.[20]

The $[M(mnt)_2]_2^{2-}$ units pack parallel to their main axis to build narrow columns surrounding the decamethylferrocenium ones. The latter are formed by quite unusual packing mode in which the $[Fe(Cp^*)_2]^+$ cations are arranged in a perpendicular manner (see Figure 1). The shortest Fe−Fe distances along the cationic row are in the range 8.38−8.40 Å whereas the anion−cation Fe−S distances observed perpendicularly are between 5.30 and 5.76(5) Å.

Structure of β-$[Fe(cp^*)_2]_2[Co(mnt)_2]_2$ (Fe_2Co_2B). The second phase in the cobalt series shows a completely different crystal structure compared to the α modification as shown in Figure 2. In the present case the compound is solvent free and the structure consists of mixed one-dimensional stacks of the dianion (A^{2-}) and cation (D^+) following the $\cdots A^{2-}D^+D^+A^{2-}D^+D^+A^{2-}\cdots$ sequence. In addition the decamethylferrocenium cations are parallel in all directions, in contrast with the first phase, and the shortest observed iron−sulfur and iron−iron distances are in the range 5.71−5.83 Å and 8.45−8.69 Å, respectively. The structure is more compact and can be described as a packing of mixed layers built by distorted centrosymmetrical hexagons of cations centered by an anionic dimer. The next layer is obtained by a one unit shift in the diagonal direction of the hexagon.

Structure of $[Fe(cp^*)_2]_2Cu(mnt)_2$ (Fe_2Cu). The geometrical parameters within $[Cu(mnt)_2]^{2-}$ and $[Fe(cp^*)_2]^+$ units are in good agreement with the reported ones.[21,22] Since the anionic unit is located on an inversion center, the average configuration is planar in contrast with the nonplanar structure reported for other compounds.[23] The crystal structure displayed in Figure 3a results from the alternance of two cations and a dianion pilled in the $\cdots A^{2-}D^+D^+A^{2-}D^+D^+A^{2-}\cdots$ sequences in the two directions of the long and short axes of the $[Cu(mnt)_2]^{2-}$ units. This packing gives rise to short anion−cation distances (*d*(Fe−S2) = 5.541(2) Å and *d*(Fe−Cu) = 6.374(1) Å. Another view of the crystal structure is displayed in Figure 3b and shows mixed stacks of dianions and $[Fe(cp^*)_2]^+$ dimers. In this case the cationic 5-fold axis is parallel to the mean plane of the anion when compared to the $[Fe(cp^*)_2]$−TCNE compound in which the 5-fold axis is perpendicular to the mean plane of the TCNE unit (TCNE = tetracyanoethylene).[22] The shortest metal−metal distances are given in Figure 3b.

Magnetic and Mössbauer Properties. For all the compounds the temperature dependence of the molar magnetic susceptibility will be represented in the form of the $\chi_M T$ versus T plot, χ_M being the molar magnetic susceptibility and T the temperature.

(18) Vasco Rodrigues, J.; Santos, I. C.; Gama, V.; Henriques, R. T.; Waerenborgh, J. C.; Duarte, M. T.; Almeida, M. *J. Chem. Soc., Dalton Trans.* **1994**, 2265.
(19) Enemark, J. H.; Lipscomb, W. N. *Inorg. Chem.* **1965**, *4*, 1729.
(20) Baker-Hawkes, M. J.; Dori, Z.; Heisenberg, R.; Gray, H. B. *J. Am. Chem. Soc.* **1968**, *90*, 4253.
(21) Plumlee, K. W.; Hoffman, B. M.; Ibers, J. A.; Soos, Z. G. *J. Chem. Phys.* **1975**, *63*, 1926.
(22) Miller, J. S.; Calabrese, J. C.; Rommelmann, H.; Chittipeddi, S. R.; Zhang, J. H.; Reiff, W. M.; Epstein, A. J. *J. Am. Chem. Soc.* **1987**, *109*, 769.
(23) Snaathorst, D.; Doesburg, H. M.; Perenboom, J. A.; Keijzers, C. P. *Inorg. Chem.* **1981**, *20*, 2526.
(24) Hendrickson, D. N.; Sohn, Y. S.; Gray, H. B. *Inorg. Chem.* **1971**, *10*, 1559.
(25) Morrison, W. H., Jr.; Krugsrud, S.; Hendrickson, D. N. *Inorg. Chem.* **1973**, *12*, 1998.
(26) Morrison, W. H., Jr.; Hendrickson, D. N. *Inorg. Chem.* **1975**, *14*, 2331.
(27) Miller, J. S.; Calabrese, J. C.; Rommelmann, H.; Chittipeddi, S. R.; Zhang, J. H.; Reiff, W. M.; Epstein, A. J. *J. Am. Chem. Soc.* **1987**, *109*, 769.

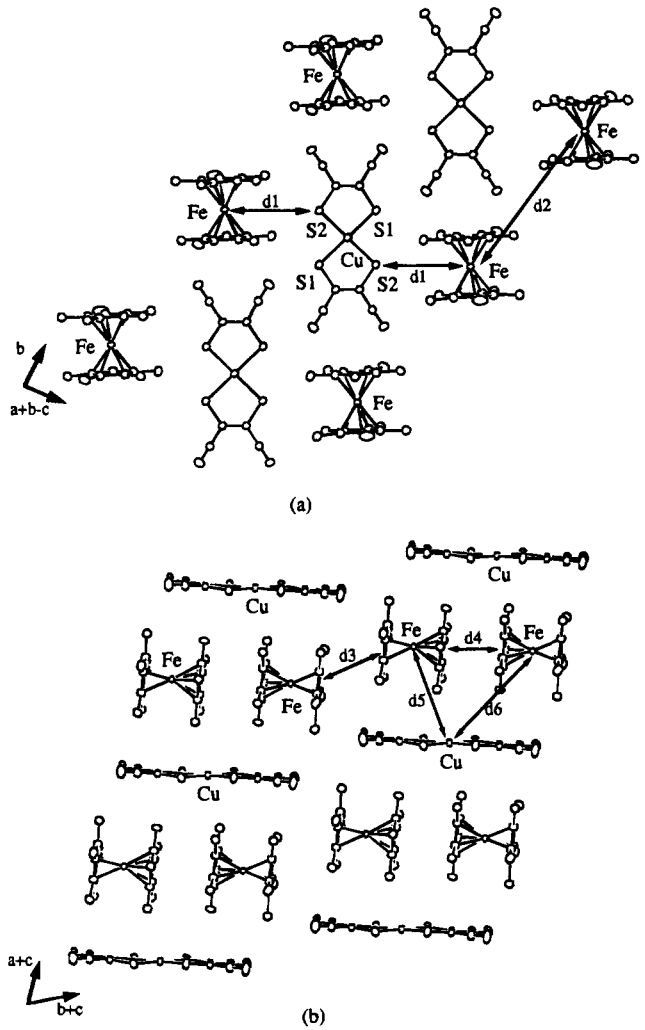

Figure 3. (a) Projection of the structure on the anionic mean plane for $[Fe(cp^*)_2]_2Cu(mnt)_2$ showing the shortest Fe−S and Fe−Fe distances: $d1 = 5.541(2)$, $d2 = 11.407(4)$ Å. (b) Structure of the mixed one-dimensional stacks for $[Fe(cp^*)_2]_2Cu(mnt)_2$ with the shortest Fe−Fe and Cu−Fe distances: $d3 = 7.843(1)$, $d4 = 7.251(1)$, $d5 = 6.374(1)$, $d6 = 7.653(1)$ Å.

α-$[Fe(cp^*)_2]_2[Co(mnt)_2]_2(CH_3CN)_2$. Mössbauer Spectra. Selected Mössbauer spectra are shown in Figure 4; fitted data are collected in Table 3.

The room-temperature spectrum contains a single, slightly asymmetric line, interpreted as an unresolved quadrupole doublet in the presence of a magnetic electronic relaxation a little faster than the magnetic hyperfine frequencies ($\sim 10^8$ Hz). These features and the hyperfine values agree with literature data on decamethylferrocenium salts.[28]

At lower temperatures, the spectra contain both a central line (sizably broader than the room-temperature line) and an extremely broad Lorentzian component, which required us to broaden the velocity scale. Such a pattern is inconsistent with a single-site relaxation line shape. However, the spectra of Fe_2Fe_2A (vide infra) will enable us unambiguously attribute the central line and the broad component to the two structural decamethylferrocenium sites.

The $\chi_M T$ versus T plot is shown in Figure 5. $\chi_M T$ is constant and equal to 1.95(3) cm^3 K mol^{-1} down to 1.7 K. The only magnetic units in this compound are the $[Fe(cp^*)_2]^+$ cations. The fact that the magnetic behavior closely follows a Curie law down to the lowest temperatures indicates that the decamethylferrocenium units do not interact within the lattice. This situation is in line with the crystal structure; along the $a + b$ direction, two nearest neighbor $[Fe(cp^*)_2]^+$ cations are separated by the very bulky diamagnetic anion $\{[Co(mnt)_2]_2\}^{2-}$. Along the $a + c$ direction, two nearest neighbor $[Fe(cp^*)_2]^+$ cations are oriented perpendicularly to each other, so that the overlap integrals of the type $\langle e_{2g}(A)|e_{2g}(B)\rangle$ between singly-occupied orbitals centered on adjacent Fe(III) centers noted A and B are all zero, which prevents any antiferromagnetic interaction. This

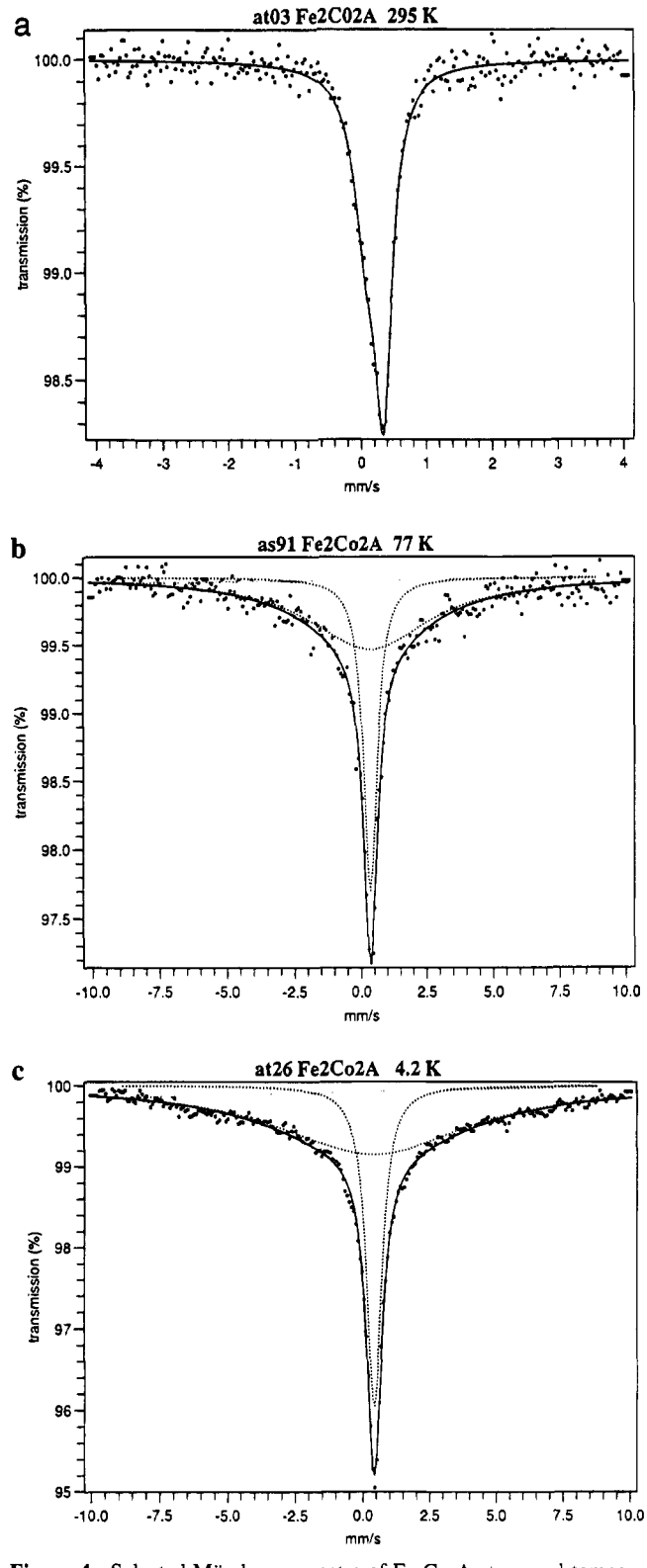

Figure 4. Selected Mössbauer spectra of Fe_2Co_2A at several temperatures and velocity ranges, with their least squares fits.

(28) Collins, R. L. *J. Chem. Phys.* **1965**, *49*, 1072.

Table 3. Least Squares Fitted Parameters of the Mössbauer Spectra for Fe_2Co_2A[a]

T	V_{max}	δ	Γ	Δ	%
amb	4	0.356(5)	0.30(1)	0.23(1)	100
			0.50(2)		
77 K	4	0.516(3)	0.73(2)	0	~42
		0.50(3)	3.6(4)	0	~58
	10	0.51(1)	0.63(3)	0	~33
			5.5(6)	0	~67
4.2 K	10	0.56(1)	0.68(1)	0	~27
			8.6(5)	0	~73

[a] Isomer shift values δ refer to metallic iron at room temperature. Γ is the half-height Lorentzian width. Δ is the quadrupole splitting. % refer to the relative areas. The standard deviations (of statistical origin) are given in parentheses.

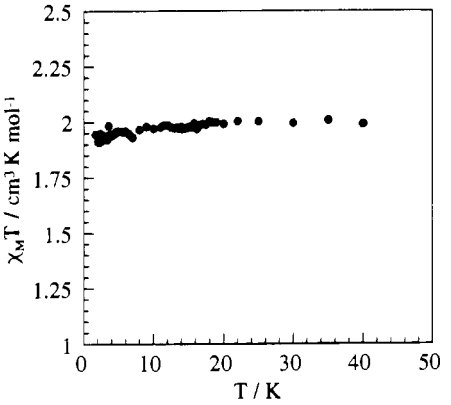

Figure 5. Temperature dependence of $\chi_M T$ for α-$[Fe(cp^*)_2]_2$-$\{[Co(mnt)_2]_2\}(CH_3CN)_2$.

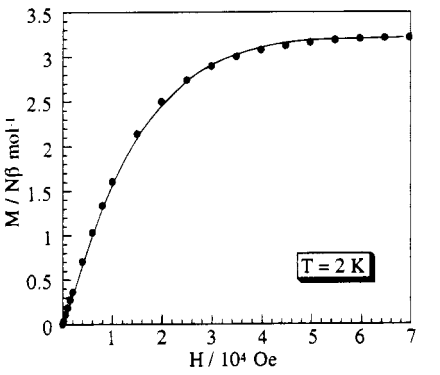

Figure 6. Field dependence of the magnetization for α-$[Fe(cp^*)_2]_2$-$\{[Co(mnt)_2]_2\}(CH_3CN)_2$ at 2 K. The full line corresponds to the Brillouin function for two local doublets (see text).

orthogonality of the magnetic orbitals could favor a ferromagnetic interaction if the overlap densities $e_{2g}(A)e_{2g}(B)$ exhibited some regions of strong magnitude, which does not happen in the present case.[4]

The Curie constant, 1.95(3) cm^3 K mol^{-1}, for two isolated local doublet states corresponds to a mean value of the g-factor equal to 3.22. This value agrees with the magnetic and EPR data of other decamethylferrocenium derivatives.[24,27]

The field dependence of the magnetization M at 2 K up to a field of 7×10^4 Oe is shown in Figure 6. The curve fits very closely the Brillouin function expected for two isolated spin doublet states with a mean value of the g-factor equal to 3.22.

The magnetic susceptibility and magnetization data for Fe_2Co_2A have nothing exceptional; however, they unambiguously show that the $[Fe(cp^*)_2]^+$ cations are magnetically isolated. They also indicate that, despite the local degeneracy of the $^2E_{2g}$ ground state, each decamethylferrocenium unit may be treated as a local spin $S = {}^1/_2$ with a g-factor equal to 3.22.

β-$[Fe(cp^*)_2]_2[Co(mnt)_2]_2$. For some obscure reasons the synthesis of this compound leads to samples which are contaminated by a small amount of ferromagnetic impurities, probably metallic iron and/or cobalt. The contribution to the observed magnetic susceptibility due to those impurities may be estimated at room temperature by measuring the field (H) dependence of the susceptibility and extrapolating to $1/H \rightarrow 0$. When doing so on different samples arising from different batches, we obtain perfect Curie law behavior in the whole 1.7–300 K temperature range with $\chi_M T$ of the order of 1.6 cm^3 K mol^{-1}. Therefore, in Fe_2Co_2B as well as in Fe_2Co_2A the decamethylferrocenium cations are magnetically isolated, which is in line with the fact that the shortest Fe- - -Fe separations are equal to 8.45 and 8.69 Å. The shortest intermolecular contacts involving the iron atoms are Fe- - -S = 5.71 and 5.83 Å. In contrast with the case of Fe_2Cu studied just below such rather short contacts do not provide any interaction pathway since the $\{[Co(mnt)_2]_2\}^{2-}$ anions have a closed-shell structure.

α-$[Fe(cp^*)_2]_2[Fe(mnt)_2]_2(CH_3CN)_2$. Mössbauer Spectra. Selected spectra are shown in Figure 7, and data collected in Table 4.

The room-temperature spectrum exhibits two components: the slightly asymmetric line due to the decamethylferrocenium units and a doublet with $S = {}^3/_2$ and $S = {}^1/_2$ possible spin states.

On the lowering of temperature, the doublet components remain unaffected, keeping narrow lines and an almost constant quadrupole splitting, as expected from literature data.[18,29,30]

To make an easier comparison to Fe_2Co_2A, we have subtracted the $[Fe(mnt)_2]_2$ doublet from the experimental spectra. The resulting "difference spectra", associated with the decamethylferrocenium contributions alone, are displayed in Figure 7e: the central line exactly behaves as in Fe_2Co_2A, with almost identical parameter values.

At 77 K, the "difference" spectrum of Fe_2Fe_2A is extremely similar to that of Fe_2Co_2A. At 4.2 K, the central line remains unaffected, but in Fe_2Fe_2A the broad component splits into a broad sextet with broad lines, typical for a striking slowing down of the electronic relaxation. (Here the fitting procedure, for convenience, used a discrete distribution of hyperfine fields,[11] which is responsible for the wavy character of the computed line shape.)

This spectacular slowing down of the electronic relaxation upon cooling can be attributed to the decrease of the effective moment of the $[Fe(mnt)_2]_2$ dimers, thus breaking magnetic couplings which ensure the fast electronic relaxation of the decamethylferrocenium units involved in the structural columns depicted in Figure 1. Very likely, the component of the spectrum drastically affected by relaxation effects must then be attributed to the decamethylferrocenium structural (Fe_1) site surrounded by the $[Fe(mnt)_2]_2$ dimers.

Magnetic Susceptibility Data. The $\chi_M T$ versus T plot is shown in Figure 8. At room temperature $\chi_M T$ is equal to 2.28 cm^3 K mol^{-1}, smoothly decreases as T decreases down to ca. 90 K, and then reaches a plateau with $\chi_M T = 1.82$ cm^3 K mol^{-1} down to 4.2 K. This low-temperature plateau for $\chi_M T$ corresponds to what is expected for two isolated $[Fe(cp^*)_2]^+$ cations. Therefore, the decrease of $\chi_M T$ in the 300–90 K temperature range is certainly due to an antiferromagnetic interaction between the two low-spin Fe(III) ions within the $\{[Fe(mnt)_2]_2\}^{2-}$ dimeric unit. This interaction is so pronounced that this entity is diamagnetic below 90 K; the triplet pair state is totally depopulated. These magnetic data agree with the Mössbauer

(29) Brichall, T.; Greenwood, N. N. *J. Chem. Soc. A* **1969**, 286.
(30) Greenwood, N. N.; Gibb, T. C. In *Mössbauer Spectroscopy*; Chapman and Hall: London, 1971; pp 206–216.

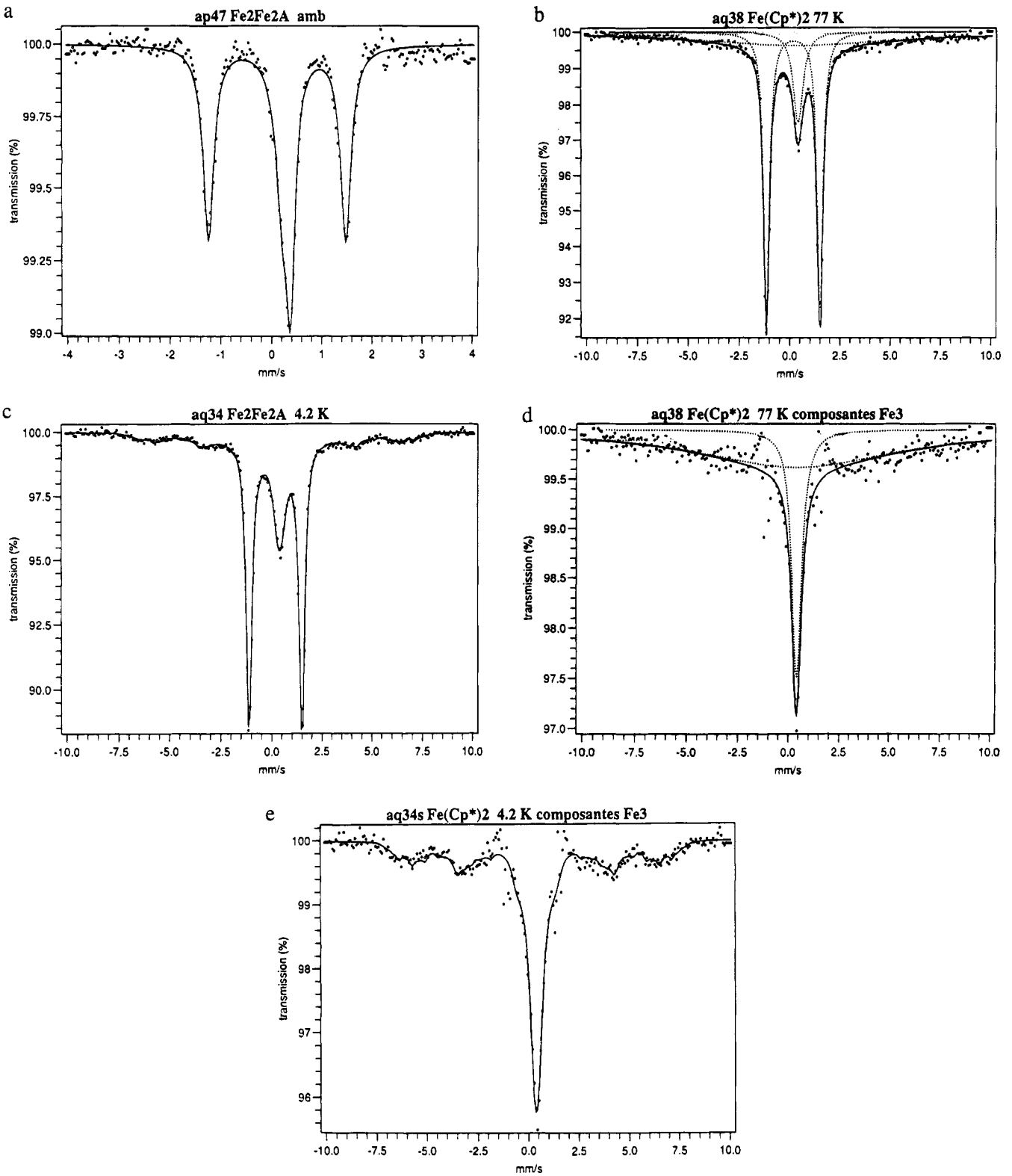

Figure 7. Selected Mössbauer spectra of Fe_2Fe_2A, at several temperatures and velocity ranges, with their least squares fits. The bottom two spectra are "difference spectra" (see text) only accounting for the ferrocenium contributions.

data discussed above. The singlet−triplet energy gap, J, within the $\{[Fe(mnt)_2]_2\}^{2-}$ anion may be easily deduced from the magnetic data. For that, $\chi_M T$ is expressed as

$$\chi_M T = C + 2N\beta^2 g^2/k[3 + \exp(-J/kT)] \qquad (1)$$

where the constant term C in the right-hand side of eq 1 refers to the two $[Fe(cp^*)_2]^+$ cations and the second term to the $\{[Fe(mnt)_2]_2\}^{2-}$ dimeric entity; g stands for the Zeeman factor of the low-spin Fe(III) ion in $\{[Fe(mnt)_2]_2\}^{2-}$. An excellent fitting of the experimental data is obtained for $J = -310\ cm^{-1}$ and $g = 2.21$. The agreement factor, defined as below, is then equal to 4×10^{-4}. It is worth emphasizing that the magnetic data do not reveal any interaction between Fe(III) ions belonging to $[Fe(cp^*)_2]^+$ and $[Fe(mnt)_2]^-$ units, respectively. This does not mean that this interaction is negligibly small. Actually, in the low-temperature range where such an interaction could influence the magnetic data, the $\{[Fe(mnt)_2]_2\}^{2-}$ dimeric entity is diamagnetic, and the spin density on each iron atom is zero.

Table 4. Least Squares Fitted Parameters of the Mössbauer Spectra for Fe_2Fe2A[a]

		Fe(mnt)$_2$ component				ferrocenium component			
T	V	δ	Γ	Δ	%	δ	Γ	Δ	%
amb	4	0.2(3)	0.26(1)	2.722(5)	52(2)	0.419(4)	0.21(1) 0.32(2)	0.17(1)	48(2)
77 K	4	0.335(2)	0.32(1)	2.630(3)	76(2)	0.558(8)	0.64(2)	0	24(2)
	10	0.34(1)	0.34(1)	2.64(1)	48(2)	0.57(1)	0.58(2) 12(2)	0	~13 ~40
4.2 K	10	0.33(1)	0.34(1)	2.62(1)	58(2)	0.53(1)	0.71(2)[b]	0 0	23(2) ~19

[a] Isomer shift values δ refer to metallic iron at room temperature. Γ is the half-height Lorentzian width. Δ is the quadrupole splitting. % refer to the relative areas. The standard deviations (of statistical origin) are given in parentheses. [b] $\langle H_{hf} \rangle$ = 35.4 T.

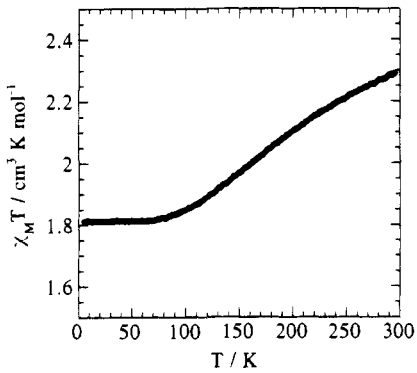

Figure 8. Experimental (■) and calculated (—) temperature dependences of $\chi_M T$ for α-[Fe(cp*)$_2$]$_2${[Fe(mnt)$_2$]$_2$}(CH$_3$CN)$_2$.

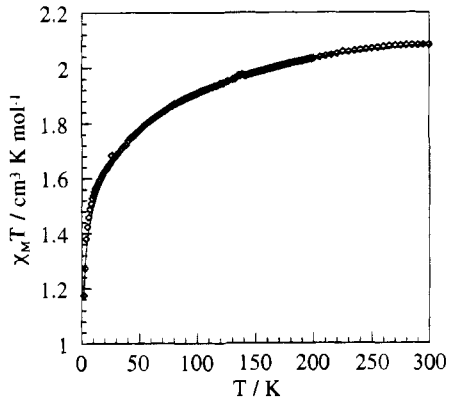

Figure 9. Experimental (◇) and calculated (—) temperature dependences of $\chi_M T$ for [Fe(cp*)$_2$]$_2$[Cu(mnt)$_2$].

[Fe(cp*)$_2$]$_2$Cu(mnt)$_2$. The $\chi_M T$ versus T plot is shown in Figure 9. At room temperature $\chi_M T$ is equal to 2.08 cm^3 K mol^{-1}, decreases first smoothly, and then more and more rapidly as T is lowered. At 1.7 K, $\chi_M T$ is equal to 1.15 cm^3 K mol^{-1}. The magnetic behavior very closely follows the Curie–Weiss law $\chi_M = 2.11/(T + 7.95)$ in the whole 1.7–300 K temperature range. The profile of the curve of Figure 9 reveals dominant antiferromagnetic interactions between the molecular units. The question we are faced with is to know whether it is possible to go further and to propose a quantitative interpretation of these susceptibility data.

We have seen that the structure of the compound shows rather short Fe- - -S contacts (5.54 Å) between a $[Cu(mnt)_2]^{2-}$ anion and two nearest neighbor $[Fe(cp^*)_2]^+$ cations. In the $[Cu(mnt)_2]^{2-}$ planar unit the spin density is strongly delocalized from the metal ion toward the sulfur atoms, which might lead to Fe- - -S interaction pathways. Neglecting all the other interactions would result in the magnetic behavior of a ABA system with $S_A = S_B = {}^1/_2$ local spins. The low-lying states for such a spin system are two doublet and one quartet states with the relative energies 0, $-J$, and $-3J/2$, respectively, J being the A–B interaction parameter occurring in the spin Hamiltonian:

$$\mathbf{H} = -J\mathbf{S}_B\cdot(\mathbf{S}_{A1} + \mathbf{S}_{A2}) \quad (2)$$

Therefore, $\chi_M T$ may be approximated as follows:

$$\chi_M T = [N\beta^2/4k)][g_{1/2,1}{}^2 + g_{1/2,0}{}^2 \exp(J/kT) + 10g_{3/2,1}{}^2 \exp(3J/2kT)]/[1 + \exp(J/kT) + 2\exp(3J/2kT)] \quad (3)$$

with[4]

$$g_{1/2,1} = (4g_A - g_B)/3$$

$$g_{1/2,0} = g_B$$

$$g_{3/2,1} = (2g_A + g_B)/3 \quad (4)$$

The minimization of the R factor defined as $\sum[(\chi_M T)^{obs} - (\chi_M T)^{cal}]^2/[(\chi_M T)^{obs}]^2$ leads to $J = -4.8$ cm^{-1}, $g_A = 3.05$, and $g_B = 1.92$. R is then equal to 7×10^{-4}, which is not a perfect theory–experiment agreement. The fitting may be improved by introducing in the expression of the magnetic susceptibility in eq 3 a Weiss constant Θ to take into account the interactions between the ABA triads. With $\Theta = 0.27$ K, R is lowered to 4×10^{-4}. The values of J, g_A, and g_B remain essentially unchanged.

Conclusion

One of our goals when we initiated this work was to design decamethylferrocenium-based molecular magnetic materials with larger dimensionality than those already reported. Another goal was to associate this larger dimensionality with interesting magnetic properties. It is indeed well-known that the onset of a long-range magnetic ordering most often is a three-dimensional property. In no case, can it be a one-dimensional effect. A series of complexes have been described all adopting a $\cdots[A_2]^{2-}D^+D^+[A_2]^{2-}D^+D^+\cdots$ or $\cdots A^{2-}D^+D^+A^{2-}D^+D^+\cdots$ molecular arrangement. The decamethylferrocenium orthogonal packing observed in the compounds Fe_2Co_2A and Fe_2Fe_2A appears interesting since it could favor ferromagnetic interactions even if, for some crucial structural reasons, such an effect between decamethylferroceniums is not observed. Nevertheless one can appreciate the fact that we are involved in a very promising field because of the structural richness and related magnetic properties of the compounds. In the present case these compounds are rather disappointing. Either the molecular units are magnetically isolated or they interact in an antiferromagnetic fashion. At this stage, one can notice that the diffuseness of the 3s and 3p sulfur orbitals enhances the overlap integrals between singly-occupied molecular orbitals (with regard, for instance, to the 2s and 2p oxygen orbitals).[31] Therefore, the

(31) Kahn, O. *Angew. Chem., Int. Ed. Engl.* **1985**, *24*, 834.

presence of sulfur atoms might favor antiferromagnetic interactions. Several decamethylferrocenium salts of nickel(III) bis(dithiolene) have been reported,[32,33] and despite the presence of ferromagnetic interactions, the ground state of these compounds is antiferromagnetic; the spin pairing interactions seem to be propagated through S- - -S contacts.

(32) Broderick, W. E.; Thomson, J. A.; Godfrey, M. R.; Sabat, M.; Hoffman, B. M. *J. Am. Chem. Soc.* **1989,** *111*, 7656.
(33) Fettouhi, M.; Ouahab, L.; Codjovi, E.; Kahn, O. *Mol. Cryst. Liq. Cryst.*, in press.

Acknowledgment. The authors thank the CNRS and the EU (Human Capital and Mobility program) for financial support of this work.

Supporting Information Available: Tables of crystal data, atomic positional and thermal parameters, anisotropic thermal parameters, bond distances, and bond angles and figures showing atom-labeling diagrams and thermal vibration ellipsoids (26 pages). Ordering information is given on any current masthead page.

IC941467B